PHYS 249 Plasma Wakefield Acceleration – Term Project: Near Critical Density Energy Scaling*

Ernesto Barraza-Valdez, Gregory B Huxtable, Gabriel Player, Danny Attiyah, Christopher Gardner, Ethan Green, Yasmeen Musthafa, Victor Flores, and Minghao Jiang
University of California, Irvine

Ilin Yeh and Khalykbek Yelshibekov
University of California, San Diego
(Dated: December 11, 2021)

The electron energy scaling with laser intensity and energy efficiency is extrapolated from 1D Particle-in-Cell Laser Wakefield Acceleration (LWFA) simulations near the critical density and compared to conventional low density LWFA scaling laws. Conventional under-dense LWFA, relies on a laser pulse length of approximately one plasma wavelength or less ($\lambda_{pulse} \approx \lambda_p$) with a group velocity near the speed of light in order to excite electrostatic plasma waves (wakes) with a similar phase velocity. Here, we examine the efficiency and maximum energy reached by electrons in traditional laser wakefield acceleration as the density approaches the critical value. Near-critical density laser wakefield has many potential applications including high dose radiation therapy.

I. INTRODUCTION

Conventional linear accelerator technology has a fundamental limit on the acceleration gradient due to electric breakdown of the materials used [1]. Thus, they require sizeable installations and complex equipment to achieve high energies [1]. Tajima and Dawson proposed using high intensity pulsed laser (10^{18} W/cm^2) to accelerate electrons with an accelerating gradient on the order of GeV/cm [2]. Their paper launched the laser wakefield acceleration (LWFA) branch of plasma physics which was further aided by the advent of Chirped Pulse Amplification (CPA) [3]. In the long history of conventional LWFA, the regime where the plasma density approaches the critical density n_c (discussed in section II) has not been thoroughly explored.

Valenta et al. determined that electron densities of roughly $0.1n_c$ were necessary for high repetition rate, low energy, short pulse lasers [4]. More recently, Nicks et al. further explored how one can achieve bulk acceleration of electrons near the critical density [5, 6]. In this paper we will further explore the parameter space near critical density LWFA and compare it to conventional underdense LWFA.

II. THEORY

To begin addressing this problem, we would first like to investigate how the the maximum energy gain of an electron, ΔE, scales with density, n_e and laser intensity a_0 in the high density regime in both relativistic ($a_0 > 1$) and non-relativistic ($a_0 < 1$) cases. Imagine a slab of uniform plasma, into which we inject a linearly polarized plane wave in the $\hat{z}$ direction.

The force felt to first order by an electron due to the laser is given by the Lorentz force:

$$F = \frac{dv_y}{dt} = \frac{qE_y}{mc} \tag{1}$$

Through a Fourier transform, we can obtain the velocity of the electron (again to first order):

$$v_y = \frac{iqE_y}{m\omega_0 c} \tag{2}$$

Thus the second order force, the ponderomotive force, becomes clear:

$$F_p = q\frac{B_z v_y}{c} = \frac{q^2 E_y}{m\omega_0 c} B_z = \frac{q^2 E_y^2}{m\omega_0 c} = m\omega_0 c a_0^2 \tag{3}$$

Where a_0 is the intensity of the laser. In the relativistic limit, F_p reduces to:

$$F_p = m\omega_0 c a_0 \tag{4}$$

The maximum energy gained by an electron from the laser is given simply by integrating the pondermotive force over half the plasma wavelength, such that:

$$\Delta E = (\frac{\pi c}{\omega_p}) F_w \gamma_{ph}^2 \tag{5}$$

where γ_{ph} is the relativistic Lorentz factor. Therefore, the maximum energy will scale quadratically or linearly, depending on the strength of the laser pulse. The Lorentz factor depends on the density as follows:

$$\begin{aligned} \gamma_{ph} = (1 - v_{ph}^2/c^2)^{-1/2} &= (1 - \omega_p^2/\omega_0^2)^{-1/2} \\ &\approx \omega_0/\omega_p = \sqrt{n_{cr}/n_e} \end{aligned} \tag{6}$$

* A footnote to the article title

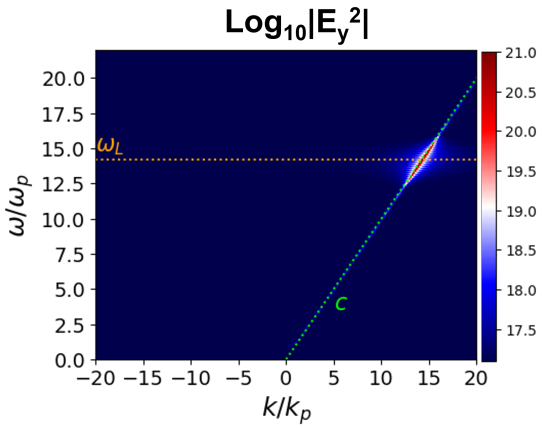

(a)

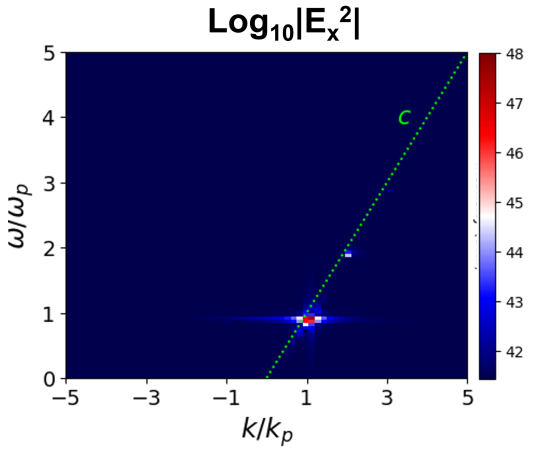

(b)

FIG. 1: Fast Fourier Transform (FFT) of the (a) transverse (E_y) and (b) longitudinal (E_x) electric field in a 1D PIC simulation of highly underdense LWFA

where ω_0 is the laser frequency, n_{cr} is the critical density for the laser, and n_e is the plasma density. This implies ΔE has a dependence on the plasma density:

$$\Delta E \propto \sqrt{n_e} \tag{7}$$

The accuracy of this relationship is what we wish to investigate.

We also wish to consider the efficiency of the laser at accelerating electrons. We define the efficiency, η, as follows

$$\eta = \mathcal{E}_{\text{plasma}}/\Delta\mathcal{E}_{\text{laser}} \tag{8}$$

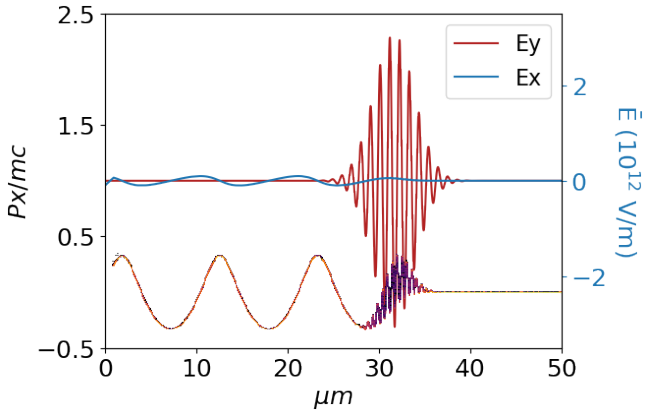

FIG. 2: Phase space plot normalized to electron mass and c on the left with the transverse (red) and longitudinal (blue) electric fields for a simulation with $a_0 = 1$ and $n_e = 0.01 \times n_{crit}$ at 150 fs.

III. UNDERDENSE VS NEAR CRITICAL DENSITY

Conventional LWFA relies on highly underdense plasma such that the plasma density is much lower than the critical density $n_e \ll n_{crit}$. Given the dispersion relation [7]:

$$\omega^2 = k^2c^2 + \omega_{pe}^2 \tag{9}$$

Where $\omega_{pe} = \sqrt{4\pi n_e e^2/m_e}$, one finds the phase velocity and group velocity to be :

$$v_{ph} = \omega/k = c\frac{\omega}{\sqrt{\omega^2 - \omega_{pe}^2}} \tag{10}$$

$$v_g = \frac{\partial\omega}{\partial k} = c\frac{\sqrt{\omega^2 - \omega_{pe}^2}}{\omega} = \frac{c}{\omega}\sqrt{1 - n_e/n_c} \tag{11}$$

In an highly underdense plasma $\omega \gg \omega_{pe}$ and both the laser phase velocity and group velocity reduce to $v_{ph} \approx v_g \approx c$. This is shown in Fig. 1a where the Fast Fourier Transform (FFT) of the transverse electric field was taken over time and plotted with respect to the frequency and wave number normalized to the plasma frequency (ω_p) and plasma wave number (k_p). When the laser's pulse width is equivalent to half the plasma wavelength: $\lambda_{pulse} = 2\pi c/(2\omega_{pe})$, then the laser's high group velocity is able to excite electrostatic (wake) waves with a similar phase velocity via the ponderomotive force described by the ponderomotive potential $\Phi = mc^2\sqrt{1 + a_0^2}$ where $a_0 = eE_0/m\omega_0 c$ is the normalized vector potential of the laser, or rather the transverse quiver velocity of the electron normalized to c. Here, E_0,ω_0 are the maximum

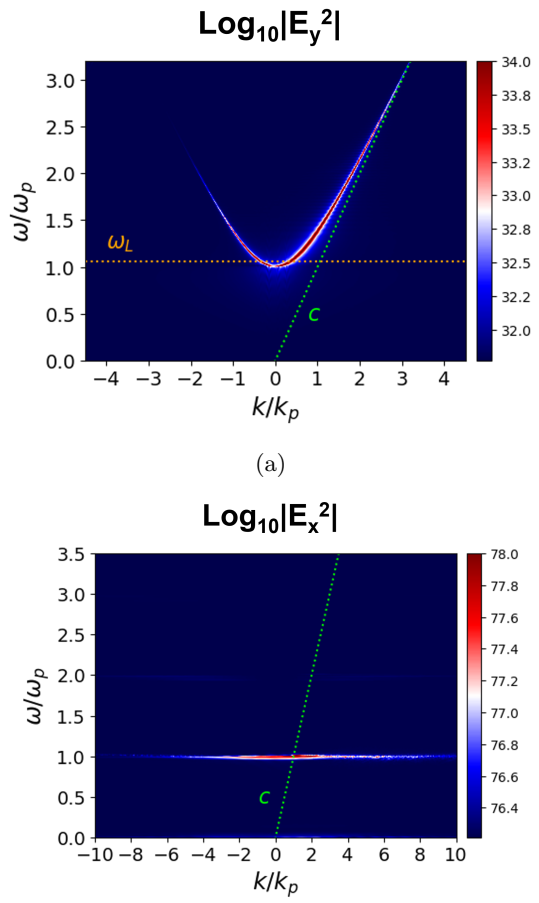

FIG. 3: Fast Fourier Transform (FFT) of the (a) transverse (E_y) and (b) longitudinal (E_x) electric field in a 1D PIC simulation of LWFA near the critical density

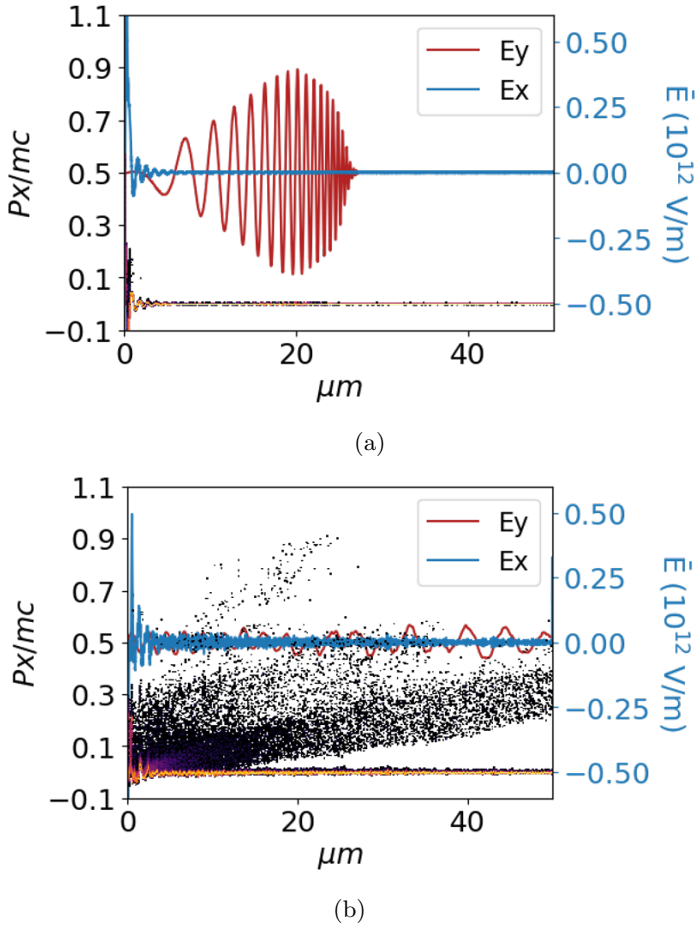

FIG. 4: Phase space plot normalized to electron mass and c on the left with the transverse (red) and longitudinal (blue) electric fields for a simulation with $a_0 = 1$ and $n_e = 0.9 \times n_{crit}$ at 100 fs (a) and 700 fs (b).

electric field and center frequency of the laser. A nonlinear effect do to the Lorentz force, the ponderomotive force drives electrons in the longitudinal direction parallel to the laser propagation. These electrons leave behind a cavity of positive charge which creates an electrostatic field polarization of magnitude:

$$E_p = m\omega_p c a_0 / e \tag{12}$$

These polarized fields then oscillate at the plasma frequency ω_p and are referred to as wake waves. In other words, for a laser frequency far above the plasma frequency, the laser propagates through the plasma unimpeded and is able to continually excite a robust train of wake waves behind it with no group velocity but a phase velocity near c as shown in Fig. 1b and Fig. 2 shows the phase space plot of that same simulation with $n_e = 0.001 \times n_{crit}$. The high group velocity of the laser and high phase velocity of the wake waves is an important aspect of the conventional LWFA because they are insulated from bulk thermal plasma instabilities where the thermal speed of the plasma can be characterized by $v_{th} = \sqrt{T/m}$

Conventional LWFA then relies on electron injection mechanisms to capture a small population of electrons and accelerate them to high energies in the train of wake waves. However, with the wake waves' high phase velocity, far away from the bulk thermal velocity, the strength of these wakes will have to grow large enough to be able to trap electrons from the fringes of the thermal distribution. The trapping width velocity is described by O'Neil [8]:

$$v_{trap} = \sqrt{qE/mk} \tag{13}$$

Where E is the amplitude of the wake wave, k is its wave number, q and m are the charge and mass of the particle to be trapped in the wake wave. Thus, because $v_{ph} \gg v_{th}$ the wakes cannot functionally trap and accelerate electrons from the bulk thermal distribution. This again reinforces that the laser and wakes are stable

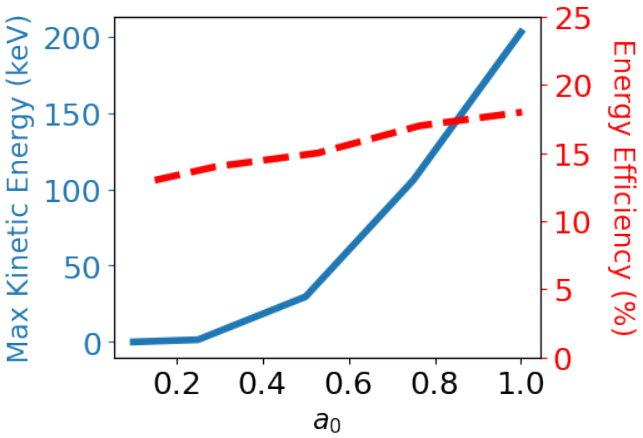

FIG. 5: The maximum electron energy (blue) 300 fs after the laser has penetrated a plasma with $n_e = 0.9 \times n_{crit}$ and laser to plasma energy efficiency (red) η vs the normalized laser vector potential (a_0).

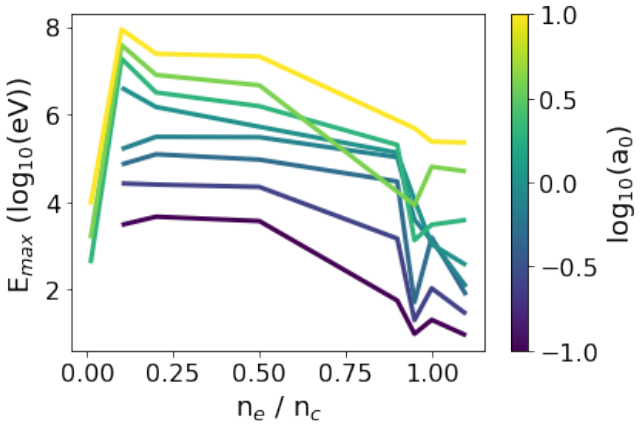

FIG. 6: The maximum kinetic energy found in simulations with respect to density and a_0.

from thermal plasma instabilities and have long coherence times.

In the limit at which the wake will begin to trap electrons from the bulk thermal distribution then $v_{trap} \sim v_{phase} \approx c \gg v_{th}$. Using Eq. (12) we find the amplitude of the wake to be:

$$E = E_{TD} = \frac{m\omega_p c}{e} \tag{14}$$

Also known as the Tajima Dawson field which is equivalent to the cold relativistic wave breaking field.

At the near critical density limit, we expect the main laser frequency to have $v_g \sim 0$. However, with the resonant condition of $\lambda_{pulse} = \lambda_p/2$ this means that near the critical density,

the laser pulse width will be single cycle or sub cycle. Thus, the frequency spectrum of the laser pulse will

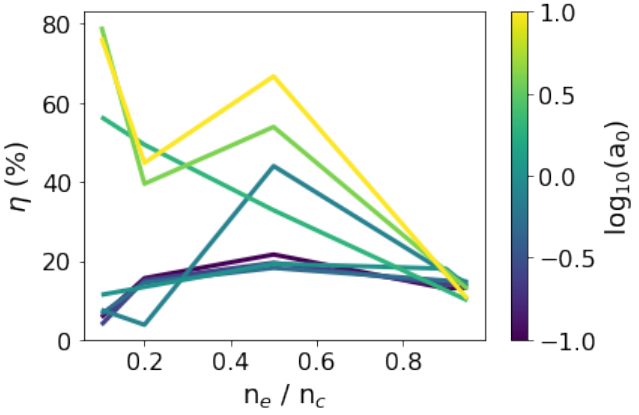

FIG. 7: The maximum efficiency (total particle energy to total laser energy) found in simulations with respect to density and a_0.

be broad bandwidth and composed of higher and lower frequencies than that of the main one.

The broad bandwidth means the laser pulse has frequency components with a varying group velocity. This is shown in FFT spectrum of Fig. 3a for a laser with a subcycle pulse width travelling through a plasma density of $n_e = 0.9 \times n_{crit}$. The varying group velocities will then cause the laser pulse to become "chirped" such that the higher frequencies race ahead of the the lower frequencies in space causing the laser pulse to broaden. This is shown in the plot 3a where the laser enters the plasma and is quickly chirped. This is opposed to the a highly underdense plasma case which allows the laser pulse to propagate without much impedance.

The broad bandwidth of the laser pulse then excites multiple electrostatic wakes at the plasma frequency (ω_p) but with different wave number values as shown in Fig. 3b. This is in contrast to the highly underdense case where coherent wake waves of a single frequency and wave number (ω_p,k_p) are excited, shown in Fig. 1b. Thus, for the near critical density case, many low phase velocity wake waves are excited which are closer to the bulk thermal distribution. These low phase velocity waves are then able to trap and accelerate low energy particles in bulk as shown in Fig. 4b phase space plot.

IV. CONCLUSION

We confirmed ΔE scales quadratically then linear from $a_0 < 1$ to $a_0 > 1$ as can be seen in Fig. 5. The efficiency shows some interesting trends including having a minimum at the critical density, and a local maximum at $n_e/n_{crit} \approx 0.5$. The local max is of interest, because there is no explicit reason as to why a local max should occur. Perhaps this may be caused from resonances with harmonics of the plasma frequency. More data points to enhance the resolution of the trends is needed to con-

firm the values of the maximums and minimums of the efficiency.

Fig. 6 shows the maximum kinetic energy found in the PIC simulations with respect to density and a_0. The trend shows a steady decline in the maximum energy as the plasma density approaches the critical density for all a_0 with a local minimum at $n_e \approx 0.95 \times n_{crit}$.

As $a_0 \to \infty$, the efficiency quickly becomes large, which is evident in Fig. 7. It is also evident that as $n \to n_c$, the efficiency η goes to zero. However, at densities near the critical, the efficiency is consistently around 15% for all a_0 values which is also confirmed by Fig. 5. Additionally there seems to be little laser-plasma interaction for low intensities ($a_0 < 0.1$) at low densities ($n_e < 0.1 \times n_{crit}$). It is generally clear that laser-driven wakefield acceleration responds positively to an increase in laser intensity and negatively to an increase in density.

[1] E. Esarey, C. B. Schroeder, and W. P. Leemans, Physics of laser-driven plasma-based electron accelerators, Rev. Mod. Phys. **81**, 1229 (2009).

[2] T. Tajima and J. M. Dawson, Laser electron accelerator, Phys. Rev. Lett. **43**, 267 (1979).

[3] D. Strickland and G. Mourou, Compression of amplified chirped optical pulses, Optics Communications **55**, 447 (1985).

[4] P. Valenta, O. Klimo, G. M. Grittani, T. Z. Esirkepov, G. Korn, and S. V. Bulanov, Wakefield excited by ultrashort laser pulses in near-critical density plasmas, in *Laser Acceleration of Electrons, Protons, and Ions V*, Vol. 11037, edited by E. Esarey, C. B. Schroeder, and J. Schreiber, International Society for Optics and Photonics (SPIE, 2019) pp. 57 – 65.

[5] B. S. Nicks, E. Barraza-Valdez, S. Hakimi, K. Chesnut, G. DeGrandchamp, K. Gage, D. Housley, G. Huxtable, G. Lawler, D. Lin, P. Manwani, E. Nelson, G. Player, M. Seggebruch, J. Sweeney, J. Tanner, K. Thompson, and T. Tajima, High-density dynamics of laser wakefield acceleration from gas plasmas to nanotubes, Photonics **8**, 10.3390/photonics8060216 (2021).

[6] T. Tajima, X. Q. Yan, and T. Ebisuzaki, Wakefield acceleration, Reviews of Modern Plasma Physics **4**, doi.org/10.1007/s41614-020-0043-z (2020).

[7] V. L. Ginzburg, *The propagation of electromagnetic waves in plasmas* (1970).

[8] T. O'Neil, Collisionless damping of nonlinear plasma oscillations, The Physics of Fluids **8**, 2255 (1965), https://aip.scitation.org/doi/pdf/10.1063/1.1761193.